

# Full-F gyrokinetic simulations of the LAPD device with open field lines and sheath boundary conditions

**Greg W. Hammett, Eric L. Shi\*, Ammar Hakim**

\* Ph.D. student who did the vast majority of the work (graduating soon)

Princeton Plasma Physics Laboratory  
Princeton University

Oxford Plasma Theory Group Seminar  
Nov. 17, 2016

(2018.09.28 corrected  
typo on p. 23, 2020.10.1  
8 corrected typos p. 21)

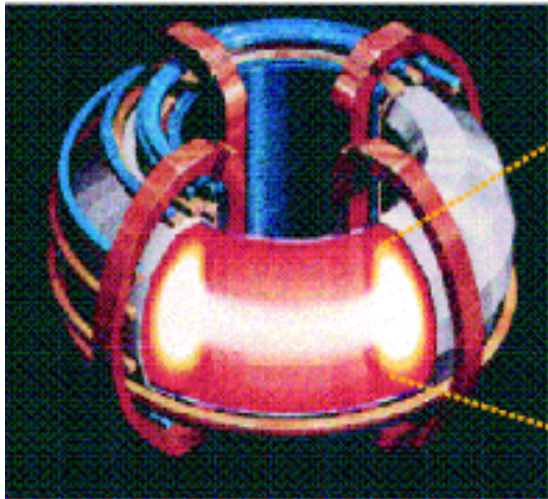
Fusion Energy 2016 IAEA paper TH/P6-2, <https://arxiv.org/abs/1610.09056>

Supported by the Max-Planck/Princeton Center for Plasma Physics, by a PPPL LDRD project, and by the DOE Scientific Discovery Through Advanced Computing (SciDAC) Program, through the Center for the Study of Plasma Microturbulence.

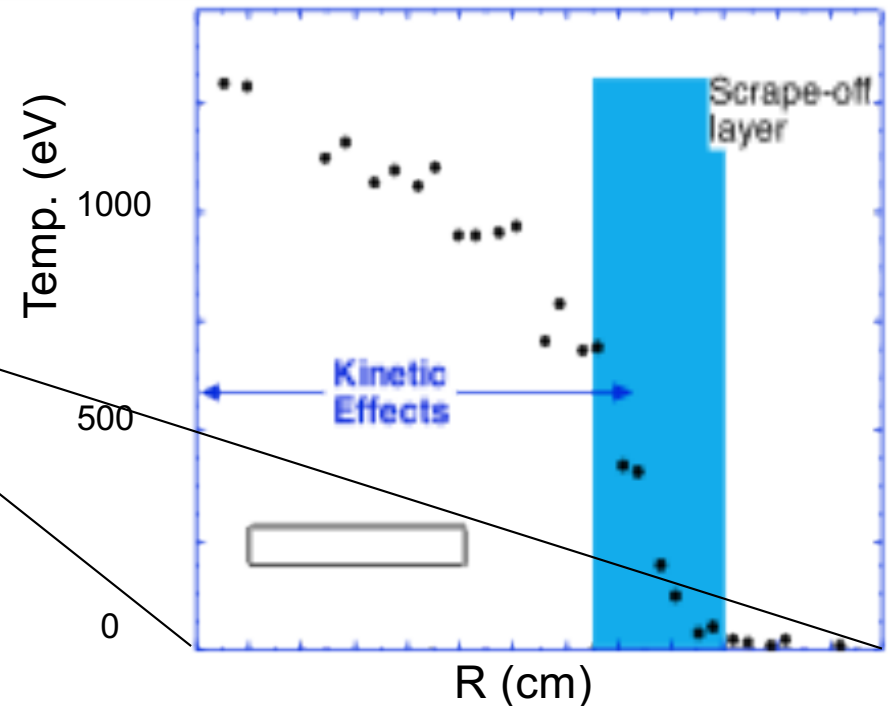
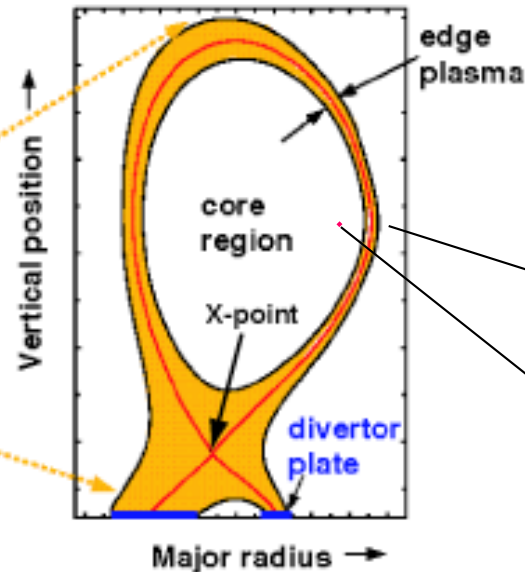


# Edge region very difficult

Tokamak magnetic fusion device



Simulated edge-plasma region



Edge pedestal temperature profile near the edge of an H-mode discharge in the DIII-D tokamak. [Porter2000]. Pedestal is shaded region.

Present core gyrokinetic codes are highly optimized for core, need new codes (or major upgrades) to handle complications of edge region of tokamaks (& stellarators):

open & closed field lines (sheath boundary conditions, plasma-wall-interactions), large amplitude fluctuations (positivity constraints, non-Maxwellian full-F), atomic physics, non-symmetric RMP/stellarator coils, magnetic fluctuations near beta limit...

Hard problem: but success of core gyrokinetic codes and progress of XGC PIC code makes us believe this is tractable, with a major initiative

# Appear to be the first continuum gyrokinetic simulations of SOL turbulence

---

- There have been a few pioneering explorations in past, but they were not continued, apparently because of various numerical difficulties
  - Pioneering work with finite-difference TEMPEST (LLNL, ~2006), focused on 4D axisymmetric neoclassical calc. Switched to 4th-order finite-volume COGENT code, better conservation/numerical properties (APS 2016: 5D slab, not yet SOL).
  - "Use of the FEFI nonlocal gyrokinetic model is planned but a sheath model compatible with violent shear Alfvén dynamics in front of the divertor plate remains to be found." (Zweben, Scott, et al., 2009)  
"Comparison of scrape-off layer turbulence in Alcator C-Mod with three dimensional gyrofluid computations", PoP, <http://dx.doi.org/10.1063/1.3191721>
- Numerical challenges of edge:
  - Large amplitude fluctuations, need  $f > 0$  (sheath instabilities if  $f < 0$  ?)
  - Conservation properties (small charge imbalances drive large potentials)
  - Stable interaction of gyrokinetics w/ sheath
  - High frequency " $\Omega_H$ " mode / "Ampere cancellation problem"?
  - Complications, but not main roadblocks: Coordinate singularities, collisions, ...
  - ...

# 2cd order Symplectic or Arakawa methods for fluids/PDEs equivalent to 2cd order Finite-Differencing

---

Advection paradigm test problem:

$$\frac{\partial F(x, t)}{\partial t} = -v \frac{\partial F}{\partial x}$$

Symplectic / Arakawa algorithm  
= standard 2cd order centered finite-difference

$$\frac{\partial F_j}{\partial t} = -v \frac{(F_{j+1} - F_{j-1}))}{2\Delta x}$$

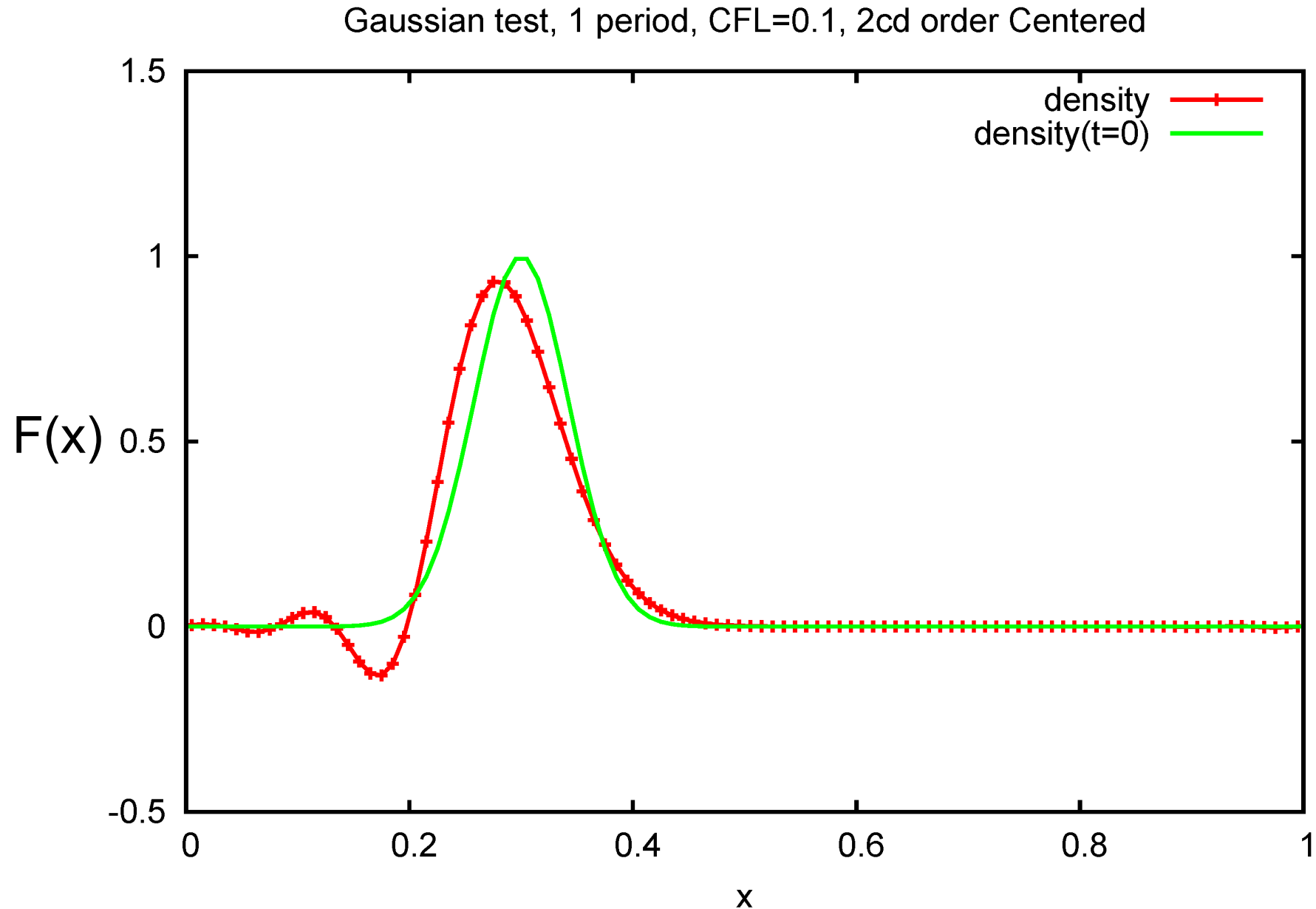
Exactly conserves particles:

$$\sum_j F_j = \text{const.}$$

and “free energy” / “entropy” /  $L_2$   
norm:

$$\sum_j F_j^2 = \text{const.}$$

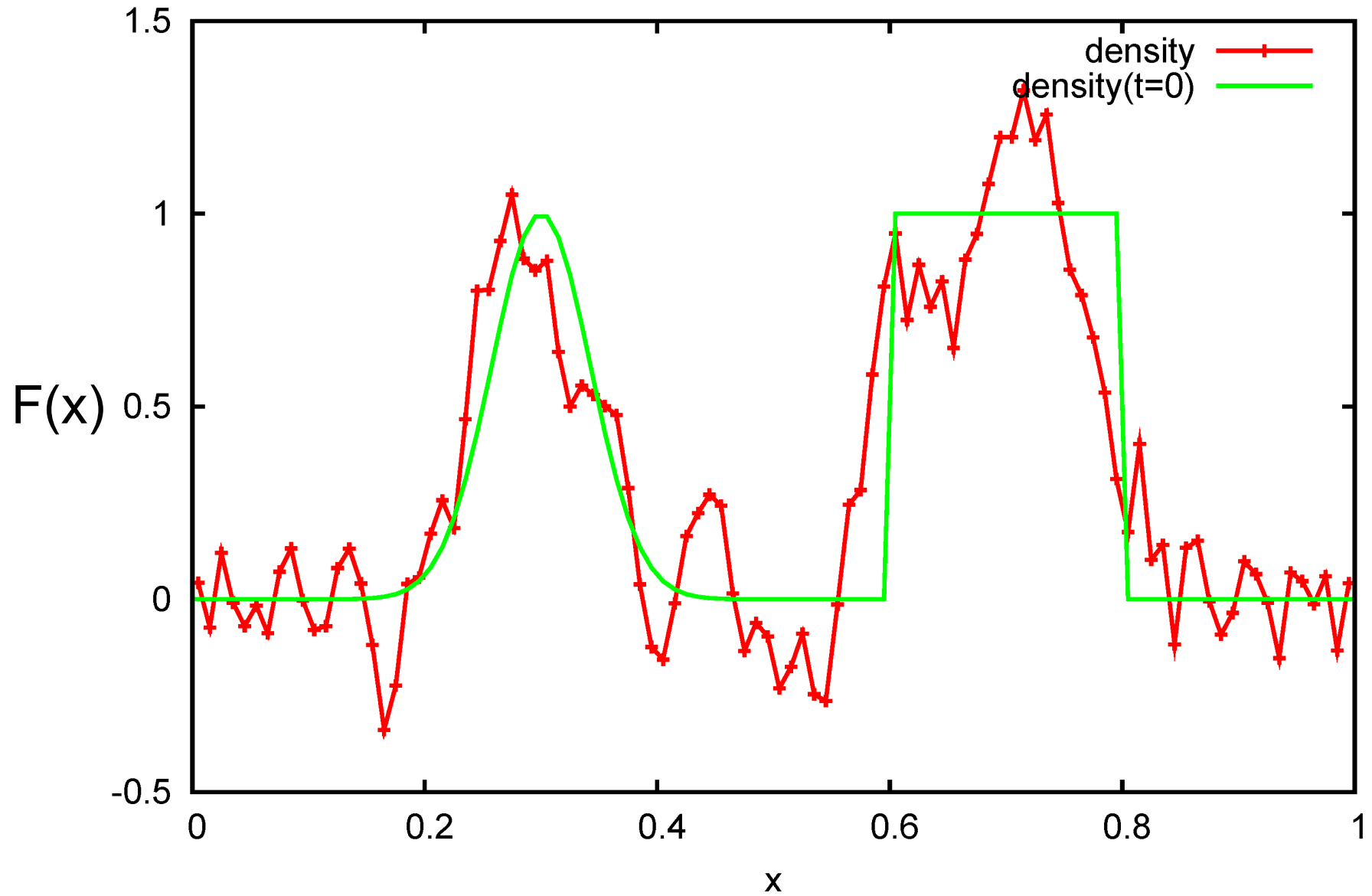
# Simple test: Advection of Gaussian pulse in periodic box



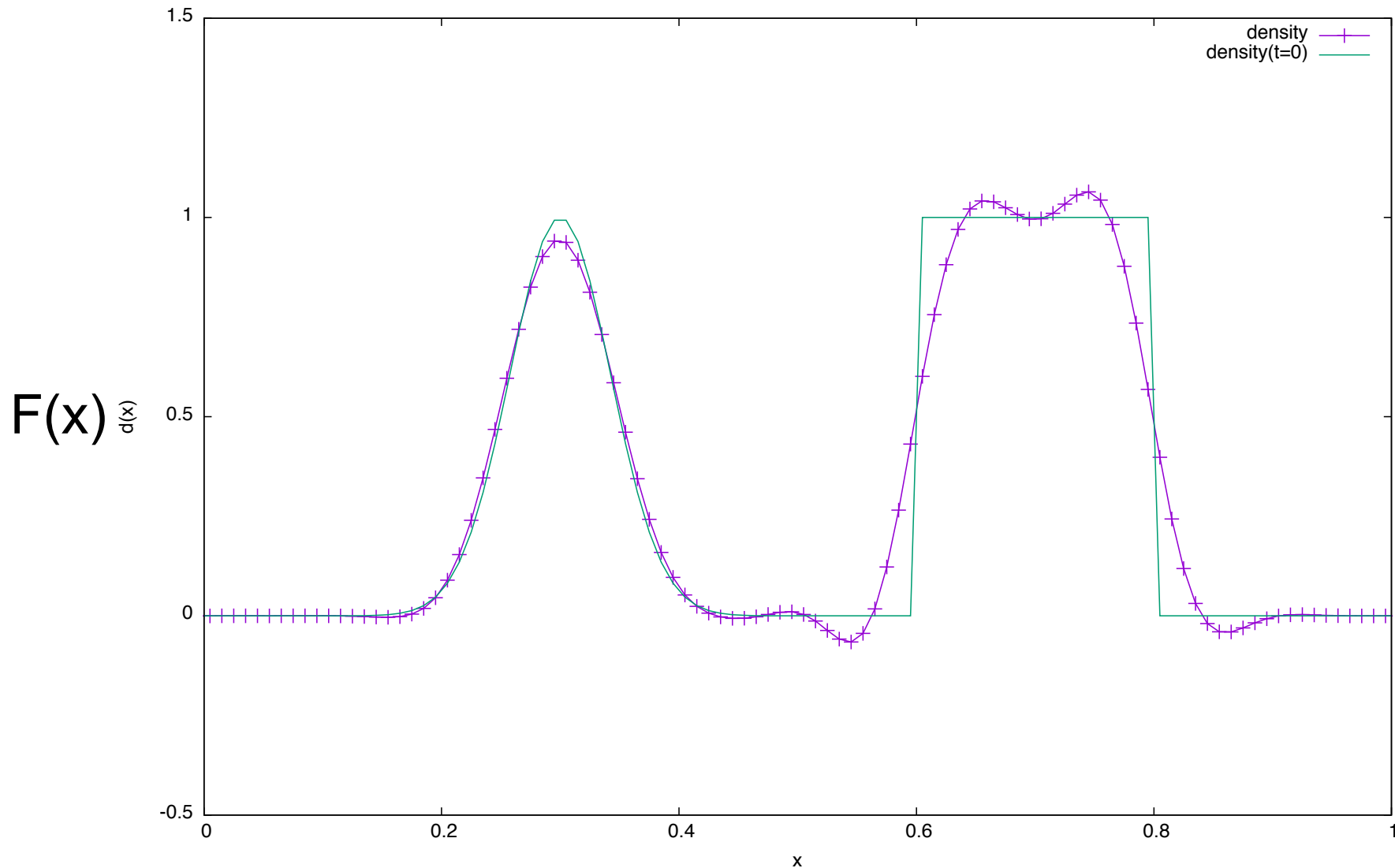
Relatively okay solution, will converge to exact solution as  $\Delta x \rightarrow 0$ . But disappointing it requires so many grid points, that there are artificial oscillations, and that  $F < 0$ .

# Harder test: Advection of Gaussian + Top Hat in periodic box

Gaussian + Step test, 1 period, CFL=0.1, 2cd order Centered



# Many common continuum algorithms (Arakawa, high-order upwind, spectral) can have difficulties in the edge

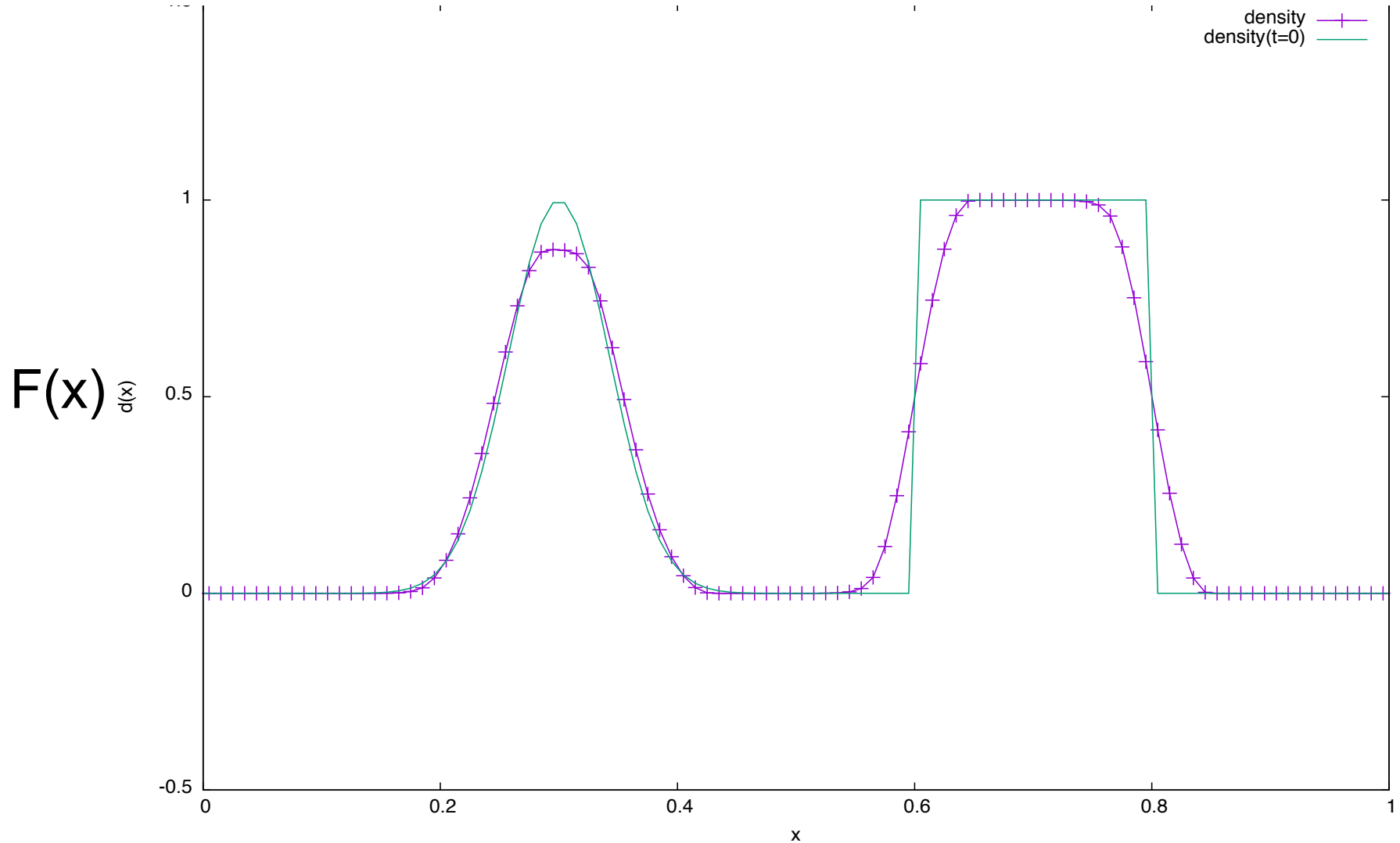


Even high-order (3<sup>rd</sup>) upwind with (hyper)diffusion has overshoots. Godunov's theorem: linear algorithm can't avoid artificial overshoots unless very diffusive 1<sup>st</sup> order upwind is used. Negative density doesn't make physical sense, could cause sheath problems.

# Nonlinear limiters developed in 1970s-1990s do fairly well

(except for some clipping of extrema)

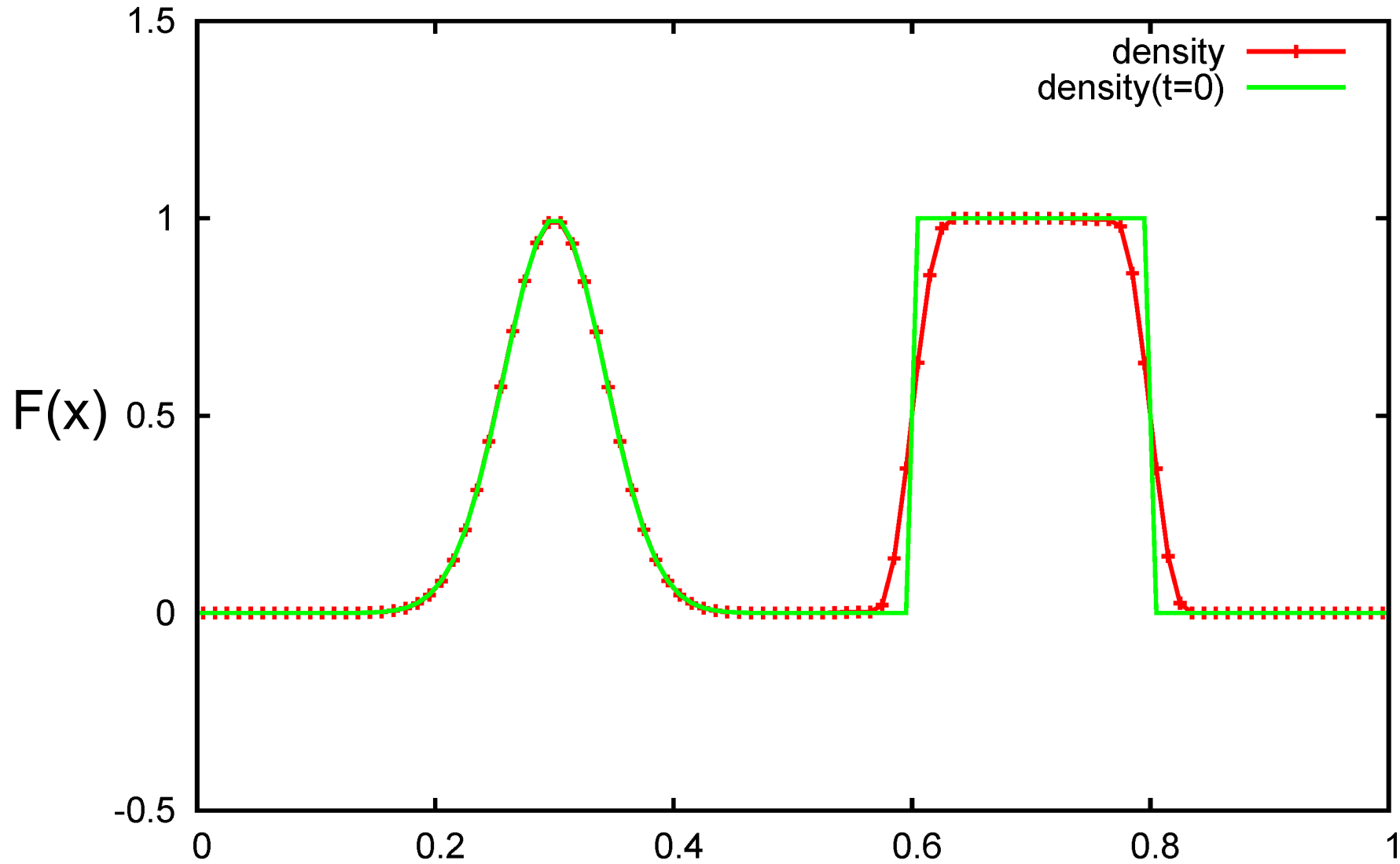
(Eliminates artificial overshoots. Gets around Godunov's theorem because of nonlinear filtering.)



Uses 3<sup>rd</sup> order initial spatial interpolation before limiter, 3<sup>rd</sup> order SSP-RK. Seems better at CFL=0.5 with 2<sup>nd</sup> order time-space-coupled time step, (exact at CFL=1), but for complex flows, will be regions at wide range of CFL= $v^*dt/dx$ , incl. CFL $\ll$ 1.

# State-of-the-Art (1997-2011) Nonlinear Limiters (Aerospace/CFD)

Introduce minimal diffusion only near sharp gradients



$x$   
Good limiters can be implemented in finite-volume (COGENT code, Dorf et al.) or DG algorithm (GKEYLL code, Shi, Hakim, Hammett). 9

# Progress & Plans for Discontinuous Galerkin Gyrokinetic Code Gkeyll

---

- Developing new gyrokinetic code using advanced continuum/Eulerian algorithms (Discontinuous Galerkin, DG) that can help with challenges of edge region of fusion devices. Want to study edge problems like the height of the pedestal, SOL width, how much improvement can be made with lithium walls. **Eventually could be a major component of a whole-device simulation using exascale computers.**
- Essential to have independent codes to cross-check each other for difficult problems.
- **Code & techniques could eventually be applied to a wider range of problems where kinetic effects become important, including astrophysics and non-plasma problems.**
- Good progress:
  - Extensive tests in lower dimensions, <http://www.ammar-hakim.org/sj/>
  - Invented several DG algorithm improvements. Improved treatment of diffusion terms: Hakim, Hammett, Shi (2014) <http://arxiv.org/abs/1405.5907>
  - Demonstrated 1D SOL Test problem of ELM on JET (*Shi et al. (Phys. Plasmas 2015)*)
  - Demonstrated ability to handle magnetic fluctuations in an efficient way.
  - Now full 3D+2v ( $x, y, z, v_{||}, v_{\perp}$ ) long-wavelength gyrokinetics in SOL (simplified helical geometry), incl. Lenard-Bernstein collisions, conducting sheath B.C.s.

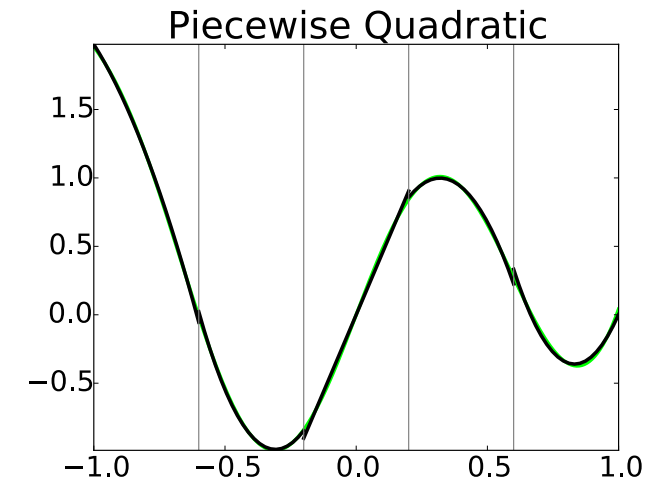
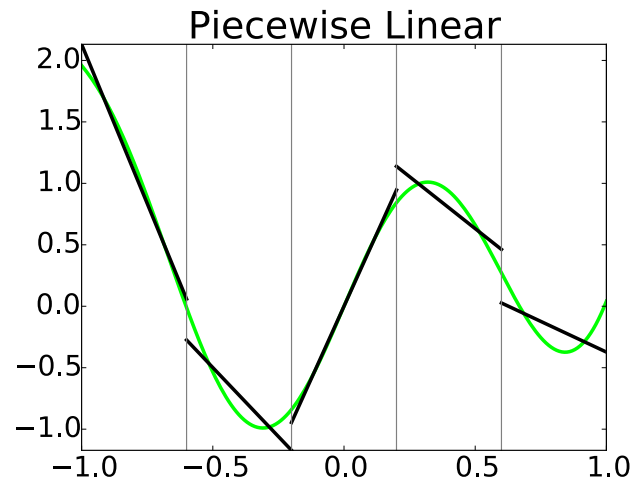
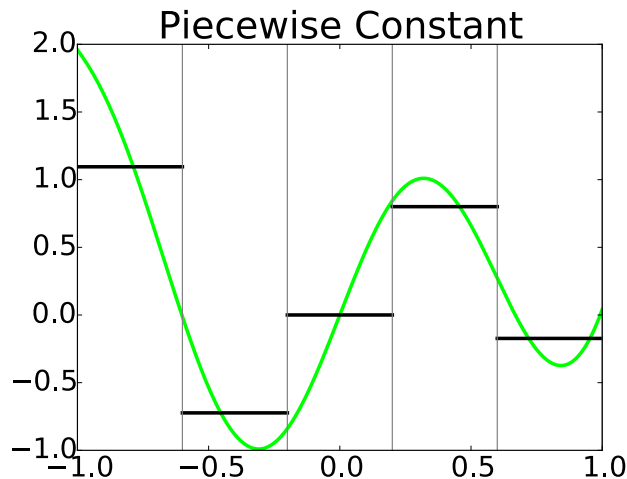
# Why consider Discontinuous Galerkin (DG) Algorithms for (Gyro)kinetics at Exascale?

---

- Higher order methods do more FLOPS to extract more out of data, need fewer data points, reduce communications that can be a bottleneck on exascale computers.
- DG allows use of limiters / upwinding to avoid negative density overshoots, which can be a major problem in the edge region of fusion devices.
- We found a version of DG that can conserve energy exactly for Hamiltonian systems like gyrokinetics, even with upwinding / limiters (for continuous time)
- DG flexibility to use Maxwellian-weighted basis functions, sparse grid ideas.
- Locality of DG means it should scale well like other continuum codes (GENE continuum code has demonstrated excellent strong scaling to 262,000 cores)
- DG: Efficient Gaussian integration --> ~ twice the accuracy / interpolation point:
  - Standard interpolation:  $p$  uniformly-spaced points to get  $p$  order accuracy
  - DG interpolates  $p$  optimally-located points to get  $2p-1$  order accuracy  
(DG has ~2x accuracy per point of Finite-Volume. We typically use  $p=2$  or  $3$ .)
- Kinetic turbulence very challenging, benefits from all tricks we can find. Potentially big win: **Factor of 2 reduction in resolution --> 64x speedup in 5D gyrokinetics**

# Discontinuous Galerkin (DG) Combines Attractive Features of Finite-Volume & Finite Element Methods

---

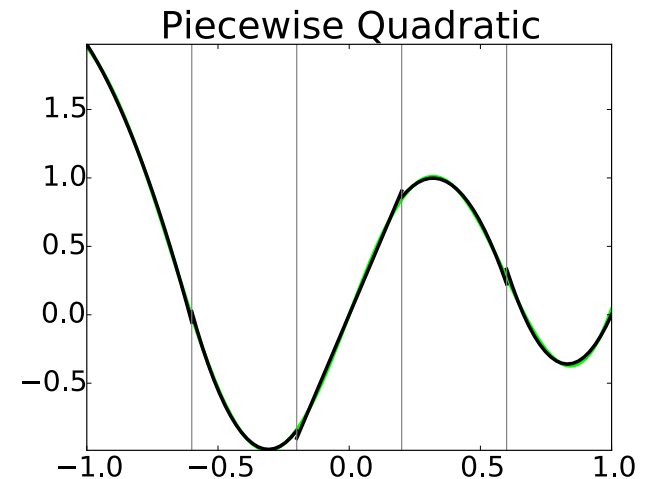
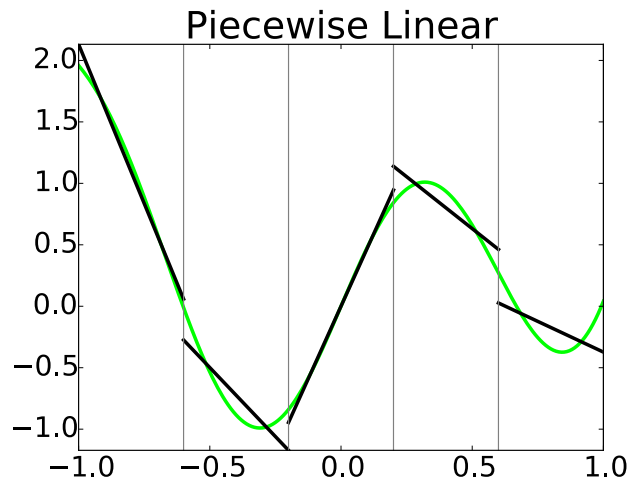
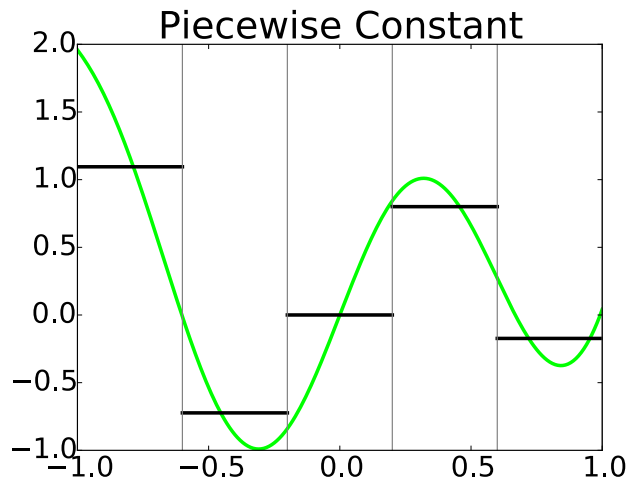


Standard finite-volume (FV) methods evolve cell averages + interpolations.

DG evolves higher-order moments in each cell. I.e. uses higher-order basis functions, like finite-element methods, but, allows discontinuities at boundary like shock-capturing finite-volume methods --> (1) easier flux limiters like shock-capturing finite-volume methods (preserve positivity) (2) calculations local so easier to parallelize.

Hot topic in CFD & Applied Math: >1500 citations to Cockburn & Shu JCP/SIAM 1998

# Discontinuous Galerkin (DG) Combines Attractive Features of Finite-Volume & Finite Element Methods



Don't get hung up on the word "discontinuous". Simplest DG is piecewise constant: equivalent to standard finite volume methods that evolve just cell averaged quantities. Can reconstruct smooth interpolations between adjacent cells when needed.

Need at least piecewise linear DG for energy conservation (conserves energy even with upwinding). Standard Finite Volume methods do not conserve energy exactly (except Arakawa, which has overshoots). Unlike Navier-Stokes fluid eqs., energy conservation in kinetic/Vlasov-Boltzmann equations is indirect, involving integration-by-parts and particle-field energy exchange.

# Standard DG Polynomial Basis Functions:

---

$$\frac{\partial f(v, t)}{\partial t} = G[f]$$

In each cell  $\Omega_j$ , expand in basis fcns:  $f(v, t) \approx f_h(v, t) = \sum_k f_k(t) b_k(v)$

Choose  $\dot{f}_k = df_k/dt$  to minimize error:  $\epsilon^2 = \int_{\Omega_j} dv \left( \sum_k \dot{f}_k b_k - G \right)^2$

Error projected into space of  $b_k(v)$  is zero:  $\int_{\Omega_j} dv b_k(v) (\dot{f}_h - G) = 0$

If  $G = -\partial\Gamma/\partial v$ , then  $b_0(v) = 1$  give density conservation:

$$\int_{\Omega_j} dv \dot{f}_h = -\Gamma(v_{j+1/2}) + \Gamma(v_{j-1/2})$$

(This is the essence of general Galerkin formulations. DG combines this with a Godunov approach of a Riemann solver / upwind fluxes at discontinuous boundaries and efficient evaluation of integrals.)

# Standard Maxwellian-Weighted DG Basis Functions:

---

For many plasma problems of interest, we know Maxwellian-weighted basis functions would be more efficient. Polynomial basis functions are ill-behaved at high  $v$ , can't integrate to  $v = \infty$ , where asymptotic behavior is Maxwellian (sometimes at higher "temperature"). Helps handle moderate collision frequencies of edge region.

$$f(v, t) \approx f_h(v, t) = \sum_k f_k(t) \underbrace{\exp(-\beta v^2 / 2) b_k(v)}_{\hat{b}_k(v)}$$

$$\text{Minimizing error leads to: } 0 = \int_{\Omega_j} dv \hat{b}_k(v) (\dot{f}_h - G)$$

But now,  $\hat{b}_0 = \exp(-\beta v^2 / 2)$  does *not* lead to standard particle conservation if  $G = -\partial\Gamma/\partial v$

$$\int_{\Omega_j} dv \hat{b}_0 \dot{f}_h = - \hat{b}_0(v) \Gamma(v) \Big|_{v_{j-1/2}}^{v_{j+1/2}} + \int_{\Omega_j} dv \frac{\partial \hat{b}_0}{\partial v} \Gamma(v)$$

Standard energy conservation doesn't hold either.

# Conservative Maxwellian-Weighted DG Basis Functions:

---

The trick for preserving conservation properties of DG with Maxwellian-weighted basis functions,  $\hat{b}_k(v) = W(v)b_k(v)$ , starts by going back to beginning, to the norm defining the error, and introducing a weighting factor:

$$\epsilon^2 = \int_{\Omega_j} dv W^{-1}(v) \left( \sum_k \dot{f}_k \hat{b}_k(v) - G \right)^2$$

Choosing  $\dot{f}_k$  to minimize error gives:

$$\int_{\Omega_j} dv W^{-1}(v) \hat{b}_m(v) \left( \sum_k \dot{f}_k \hat{b}_k - G \right) = 0$$

$$\int_{\Omega_j} dv b_m(v) \left( \sum_k \dot{f}_k \hat{b}_k - G \right) = 0$$

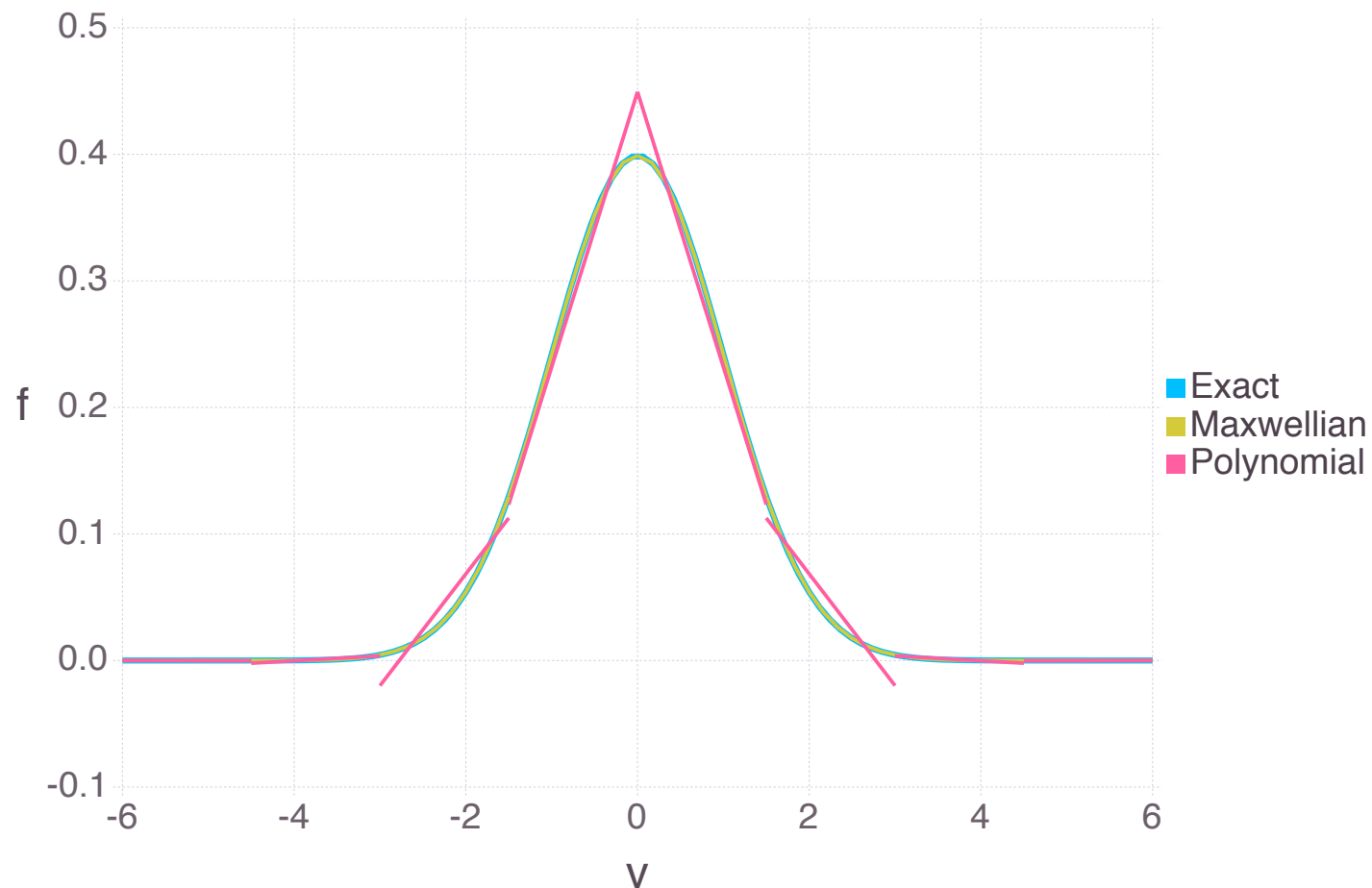
Now  $b_0(v) = 1$  gives standard particle conservation. Higher moments give momentum and energy conservation for collision operator (Hamiltonian terms more complicated..., see A. Hakim's poster.)

Weighted DG can be thought of as Petrov-Galerkin, test fncs  $\neq$  basis fncs

# Collision Operator Benchmark

Compare Maxwellian-weighted and polynomial basis functions by solving the equation (Lenard-Bernstein collision operator)

$$\frac{\partial f}{\partial t} = C[f] = \nu \frac{\partial}{\partial v_{\parallel}} \left( v_{\parallel} f + v_T^2 \frac{\partial f}{\partial v_{\parallel}} \right)$$



# Example Using Local Maxwellian Parameters

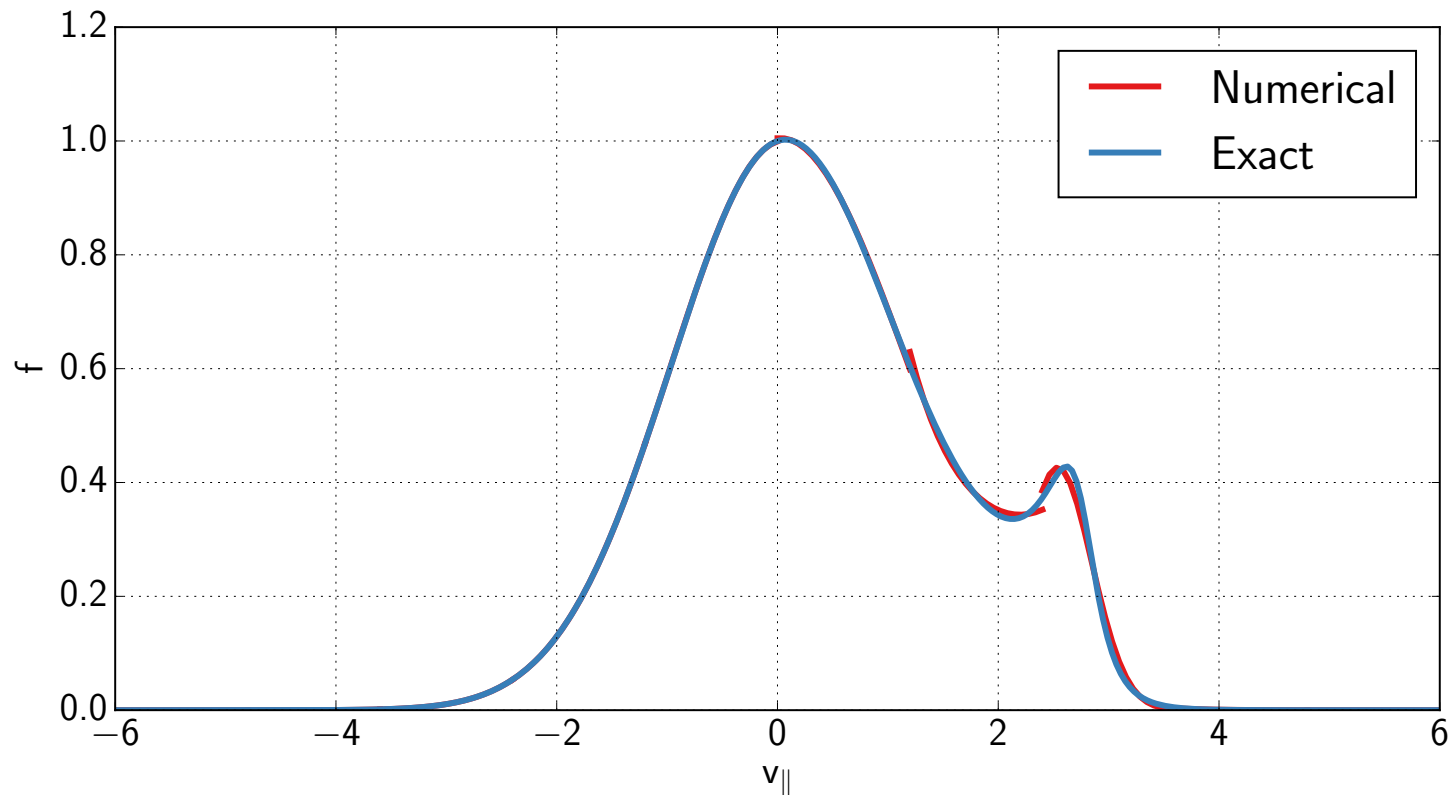


**Figure:** The local Maxwellian parameter calculation is applied to discretize a function including a non-monotonic bump to demonstrate the ability to handle strongly non-Maxwellian functions.

(Similar to Gaussian Radial Basis Functions but conserves energy and applied only piecewise in velocity)

# 1D Test problem: Classical Parallel Heat Conduction

---

$$\frac{\partial f(z, v_{\parallel}, t)}{\partial t} + v_{\parallel} \frac{\partial f}{\partial z} = C[f]$$

Background temperature gradient (w/ force balance), Chapman-Enskog-Braginskii problem locally becomes equivalent to 1D problem:

$$\frac{\partial f(v_{\parallel}, t)}{\partial t} = C[f] + \kappa_T v_{\parallel} \left( \frac{1}{2} \frac{v_{\parallel}^2}{v_t^2} - c_1 \right) f$$

( $\kappa_t \ll 1$ .  $c_1$  determined by constraint of no momentum injection.)

Lenard-Bernstein Collision model (much better than Krook model for plasmas):

$$C[f] = \frac{\partial}{\partial v_{\parallel}} \left( \nu v_{\parallel} f + \nu v_t^2 \frac{\partial f}{\partial v_{\parallel}} \right)$$

Solve to steady state, calculate heat flux =  $\int dv_{\parallel} (1/2) m v_{\parallel}^3 f$ .

# Maxwellian-weighted basis functions much more efficient

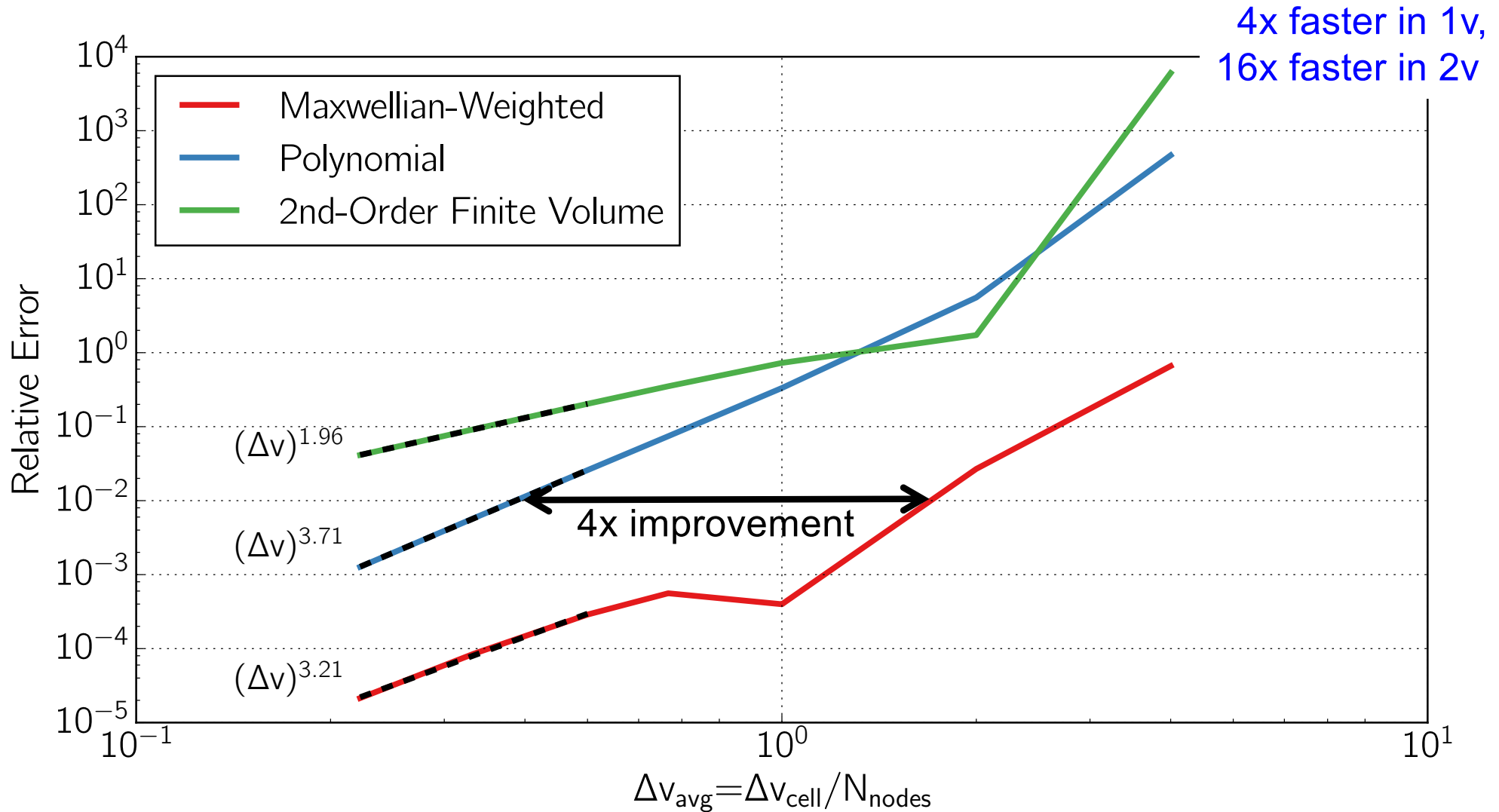


Figure: Relative error in heat flux calculation for cases of varying cell width, keeping  $v_{\text{max}} = 8v_T$ .

(Exponential-weighted basis functions not yet implemented in main Gkeyll code, but utility demonstrated in standalone code.)

# Energy Balance in full F GK (with linear polarization):

For simplicity, consider long-wavelength full-F gyrokinetics, curvature drifts turned off, and time-independent dielectric coefficient  $\epsilon_{\perp 0}(x) = c^2/v_A^2 = c^2 4\pi \sum_s n_0(x) m/B^2$  :

$$\frac{\partial f}{\partial t} + \frac{\partial}{\partial z} (v_{\parallel} f) + \nabla \cdot (\vec{v}_E f) + \frac{\partial}{\partial v_{\parallel}} \left( \frac{q}{m} E_{\parallel} f \right) = C[f] + S$$

$$-\nabla_{\perp} \cdot (\epsilon_{\perp 0} \nabla_{\perp} \phi) = 4\pi \sigma_{gc} = 4\pi \sum_s q \int d^3 v f \quad \text{(guiding center charge + polarization charge = 0)}$$

Can write the GK equation in Hamiltonian form with  $H = \frac{1}{2} m v_{\parallel}^2 + q\phi$

$$\frac{\partial f}{\partial t} = \{H, f\} + C[f] + S$$

$$\{H, f\} = \frac{\partial H}{\partial z} \frac{1}{m} \frac{\partial f}{\partial v_{\parallel}} - \frac{1}{m} \frac{\partial H}{\partial v_{\parallel}} \frac{\partial f}{\partial z} - \frac{c}{qB} \left( \frac{\partial H}{\partial x} \frac{\partial f}{\partial y} - \frac{\partial H}{\partial y} \frac{\partial f}{\partial x} \right)$$

Can show conserved total energy (in a periodic domain with no sources) is:

$$\begin{aligned} W_{\text{tot}} &= \int d^3 x \sum_s \int d^3 v f H - \int d^3 x \frac{\epsilon_{\perp 0}}{8\pi} |\nabla_{\perp} \phi|^2 \\ &= W_{\parallel} + \int d^3 x \sigma \phi - \int d^3 x \sum_s n_0 \frac{1}{2} m v_E^2 \\ &= W_{\parallel} + \int d^3 x \sum_s n_0 \frac{1}{2} m v_E^2 \end{aligned}$$

## Proof (fill in the details as homework):

In first term of  $dW_{tot}/dt$ ,

$$\begin{aligned}\frac{dW_H}{dt} &= \int d^3x \sum_s \int d^3v \left( \frac{\partial f}{\partial t} H + f \frac{\partial H}{\partial t} \right) \\ &= \int d^3x \sum_s \int d^3v \left( \{H, f\} H + f q \frac{\partial \phi}{\partial t} \right) \\ &= \int d^3x \sum_s \int d^3v \left( \frac{1}{2} \{H^2, f\} + f q \frac{\partial \phi}{\partial t} \right) \\ &= \int d^3x \sigma_{gc} \frac{\partial \phi}{\partial t} \\ &= - \int d^3x \nabla_{\perp} \cdot \left( \frac{\epsilon_0}{4\pi} \nabla_{\perp} \phi \right) \frac{\partial \phi}{\partial t} \\ &= \frac{d}{dt} \int d^3x \frac{\epsilon_0}{8\pi} |\nabla_{\perp} \phi|^2 \\ &= \frac{d}{dt} \int d^3x \sum_s n_0 \frac{1}{2} m v_E^2\end{aligned}$$

# Energy Balance in full F GK (with nonlinear polarization)

In the edge/SOL region, there are large density fluctuations on the time scale of the turbulence, so can't assume  $n(\mathbf{x},t)$  factor in polarization density is independent of time. Generalize to time-dependent dielectric coefficient  $\epsilon_{\perp}(\mathbf{x},t) = c^2/v_A^2 = c^2 4\pi \sum_s n(\mathbf{x},t) m/B^2$  :

$$-\nabla_{\perp} \cdot (\epsilon_{\perp} \nabla_{\perp} \phi) = 4\pi \sigma_{gc} = 4\pi \sum_s q \int d^3v f$$

General Poisson-bracket form of GK eq. unchanged, but Hamiltonian modified to include a second order contribution:

$$H = \frac{1}{2} m v_{\parallel}^2 + q\phi - \frac{1}{2} m v_E^2$$

As described in papers by Sugama, Brizard, Scott, Krommes, et al., in a field-theory approach to GK one needs 2cd order contributions to  $H$  that scale as  $\phi^2$ , so taking variations w.r.t.  $\phi$  leads to the term in the GK Poisson equation that is linear in  $\phi$ .

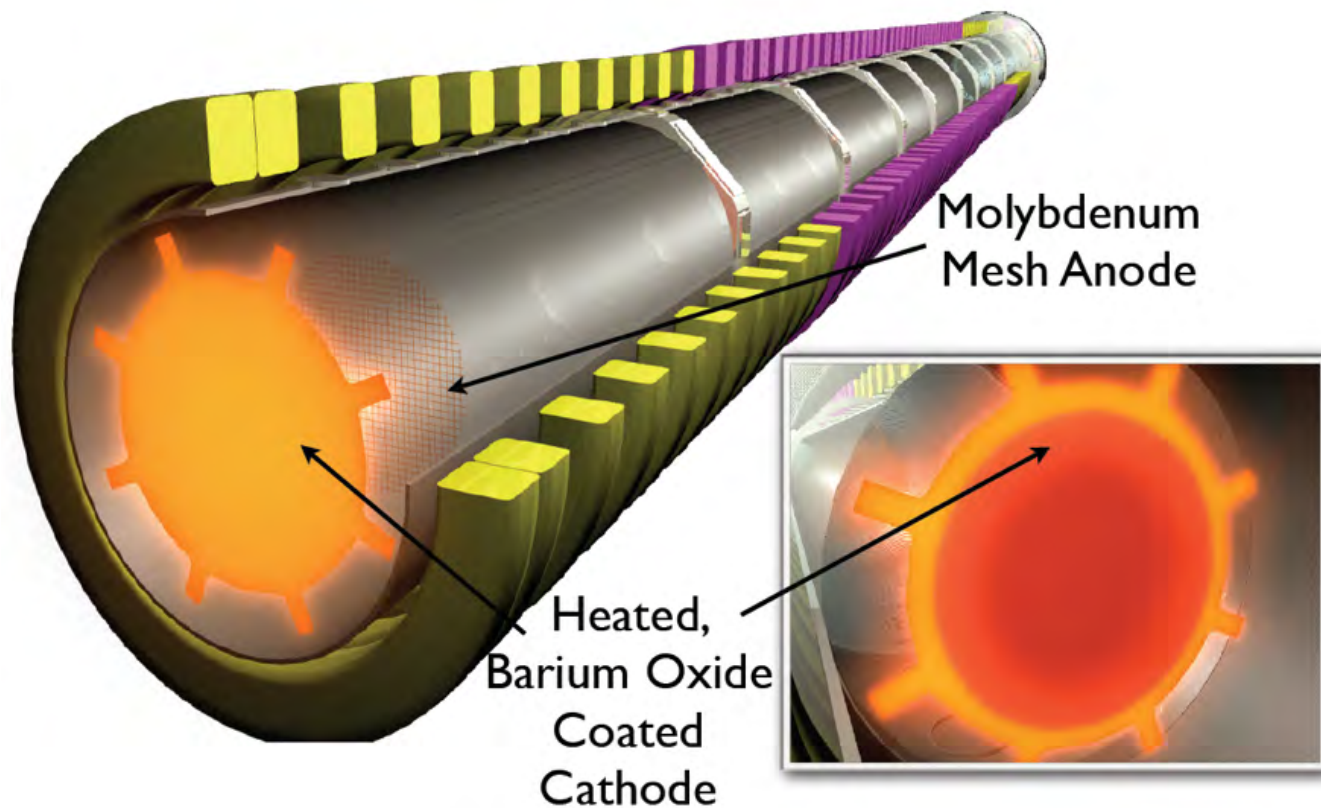
Now the conserved total energy is just:

$$\begin{aligned} W_{\text{tot}} &= \int d^3x \sum_s \int d^3v f H \\ &= W_{\parallel} + \int d^3x \sigma \phi - \int d^3x \sum_s n \frac{1}{2} m v_E^2 \\ &= W_{\parallel} + \int d^3x \sum_s n \frac{1}{2} m v_E^2 \end{aligned}$$

(typo corrected:  $n$  had been  $n_0$ .)

# First 5D Continuum Gyrokinetic Simulations with With Gkeyll w/ Open Field Lines & Sheath b.c.

## LAPD Plasma source



Builds on earlier pioneering fluid simulations of LAPD by Rogers and Ricci (predecessor to GBS code), and by Umansky, Friedman, et al. (BOUT++).

## Low-Frequency Turbulence in a Linear Magnetized Plasma

B. N. Rogers<sup>1,\*</sup> and Paolo Ricci<sup>2,†</sup>

<sup>1</sup>*Department of Physics and Astronomy, Dartmouth College, Hanover, New Hampshire 03755, USA*

<sup>2</sup>*Centre de Recherches en Physique des Plasmas–École Polytechnique Fédérale de Lausanne, Association EURATOM-Confédération Suisse, CH-1015 Lausanne, Switzerland*

(Received 23 March 2010; published 2 June 2010)

Plasma turbulence in a linear device is explored for the first time with three-dimensional global two-fluid simulations, focusing on the plasma parameters of the Large Plasma Device. Three instabilities are present in the simulations: the Kelvin-Helmholtz instability, a sheath-driven instability, and a resistive drift wave instability. The Kelvin-Helmholtz mode is shown to dominate the transport of plasma across the magnetic field. Simple scaling laws are obtained for the plasma profiles.

DOI: 10.1103/PhysRevLett.104.225002

PACS numbers: 52.35.Ra, 52.30.Ex, 52.35.Kt

Linear plasma devices (e.g., [1–6]) are of widespread interest to the plasma physics community because they allow the exploration of basic plasma phenomena without the complexities of magnetic curvature and shear. Of particular interest in this work, the Large Plasma Device (LAPD) experiment [1] creates a linear plasma approximately 18 m long and 30 cm in radius with straight magnetic field lines that terminate on the end walls. Among its many uses, this experiment has been applied to the study of turbulence and transport [7–11] due to modes such as the Kelvin-Helmholtz (KH) instability and drift waves. These modes are of high interest because they are ubiquitous in magnetized plasmas, and drift waves, in particular, are believed to play a central role in the edge region of fusion devices. The latter topic is of great importance to the fusion community because edge turbulence largely governs the overall fusion performance of tokamaks and similar machines.

rium electric potential arising from the sheath boundary conditions [13]:  $e\phi \approx \Lambda T_e$ , where  $\Lambda = \log\sqrt{m_i/(2\pi m_e)} \approx 3$ . The nonlinear evolution of the KH mode produces large-scale eddies that are the main source of cross-field profile relaxation.

For our study we use the electrostatic Braginskii equations [14] with  $T_i \ll T_e$  and  $\beta \ll 1$ :

$$\frac{dn}{dt} = -\frac{\partial(nV_{\parallel e})}{\partial z} + S_n, \quad \frac{dV_{\parallel i}}{dt} = -V_{\parallel i} \frac{\partial V_{\parallel i}}{\partial z} - \frac{1}{n} \frac{\partial p_e}{\partial z}, \quad (1)$$

$$\frac{d\nabla_{\perp}^2 \phi}{dt} = -V_{\parallel i} \frac{\partial \nabla_{\perp}^2 \phi}{\partial z} + \frac{m_i \Omega_{ci}^2}{e^2 n} \frac{\partial j_{\parallel}}{\partial z}, \quad (2)$$

$$\frac{dT_e}{dt} = \frac{2}{3} \frac{T_e}{en} 0.71 \frac{\partial j_{\parallel}}{\partial z} - \frac{2}{3} T_e \frac{\partial V_{\parallel e}}{\partial z} - V_{\parallel e} \frac{\partial T_e}{\partial z} + S_T, \quad (3)$$

$$m_e \frac{dV_{\parallel e}}{dt} = -m_e V_{\parallel e} \frac{\partial V_{\parallel e}}{\partial z} - \frac{T_e}{n} \frac{\partial n}{\partial z} + e \frac{\partial \phi}{\partial z} - 1.71 \frac{\partial T_e}{\partial z} + \frac{ej_{\parallel}}{n},$$

For our study we use the electrostatic Braginskii equations [14] with  $T_i \ll T_e$  and  $\beta \ll 1$ :

$$\frac{dn}{dt} = -\frac{\partial(nV_{\parallel e})}{\partial z} + S_n, \quad \frac{dV_{\parallel i}}{dt} = -V_{\parallel i} \frac{\partial V_{\parallel i}}{\partial z} - \frac{1}{n} \frac{\partial p_e}{\partial z}, \quad (1)$$

$$\frac{d\nabla_{\perp}^2 \phi}{dt} = -V_{\parallel i} \frac{\partial \nabla_{\perp}^2 \phi}{\partial z} + \frac{m_i \Omega_{ci}^2}{e^2 n} \frac{\partial j_{\parallel}}{\partial z}, \quad (2)$$

$$\frac{dT_e}{dt} = \frac{2}{3} \frac{T_e}{en} 0.71 \frac{\partial j_{\parallel}}{\partial z} - \frac{2}{3} T_e \frac{\partial V_{\parallel e}}{\partial z} - V_{\parallel e} \frac{\partial T_e}{\partial z} + S_T, \quad (3)$$

$$m_e \frac{dV_{\parallel e}}{dt} = -m_e V_{\parallel e} \frac{\partial V_{\parallel e}}{\partial z} - \frac{T_e}{n} \frac{\partial n}{\partial z} + e \frac{\partial \phi}{\partial z} - 1.71 \frac{\partial T_e}{\partial z} + \frac{e j_{\parallel}}{\sigma_{\parallel}}, \quad (4)$$

where  $p_e = nT_e$ ,  $[a, b] = \partial_x a \partial_y b - \partial_y a \partial_x b$ ,  $df/dt = \partial f / \partial t - (c/B)[\phi, f]$ ,  $j_{\parallel} = en(V_{\parallel i} - V_{\parallel e})$ ,  $\Omega_{ci} = eB/(m_i c)$ . The  $z$  is the coordinate parallel to  $B$ . We solve Eqs. (1)–(4) on a field-aligned grid using a finite difference scheme with Runge-Kutta time stepping and small numerical diffusion terms. The computational domain has a rectangular shape spanning  $(-L/2, L/2)$ ,  $L = 100\rho_{s0}$  in the perpendicular directions and  $(-L_z/2, L_z/2)$  in the parallel

ually no plasma reaches the walls and thus the transverse boundary conditions have no impact on the simulations. This simplifies the simulations but is different from the experiments, which have a somewhat smaller circular cross section ( $\sim 1$  m diameter). Another simplification concerns the sources: in the simulations the sources are uniform in the parallel direction, and standard Bohm boundary conditions  $V_{\parallel i} = \pm c_s$ ,  $V_{\parallel e} = \pm c_s \exp(\Lambda - e\phi/T_e)$  are applied at the end walls  $z = \pm L_z/2$ . In the LAPD experiments, however, the situation is more complicated. Energetic electrons are injected by an anode-cathode arrangement at one end [1], and the potential of the anode and cathode can be biased relative to the walls of the vacuum chamber. Data can be taken during the active period of the

# Fluid Simulations of LAPD (Rogers & Ricci PRL 2010)

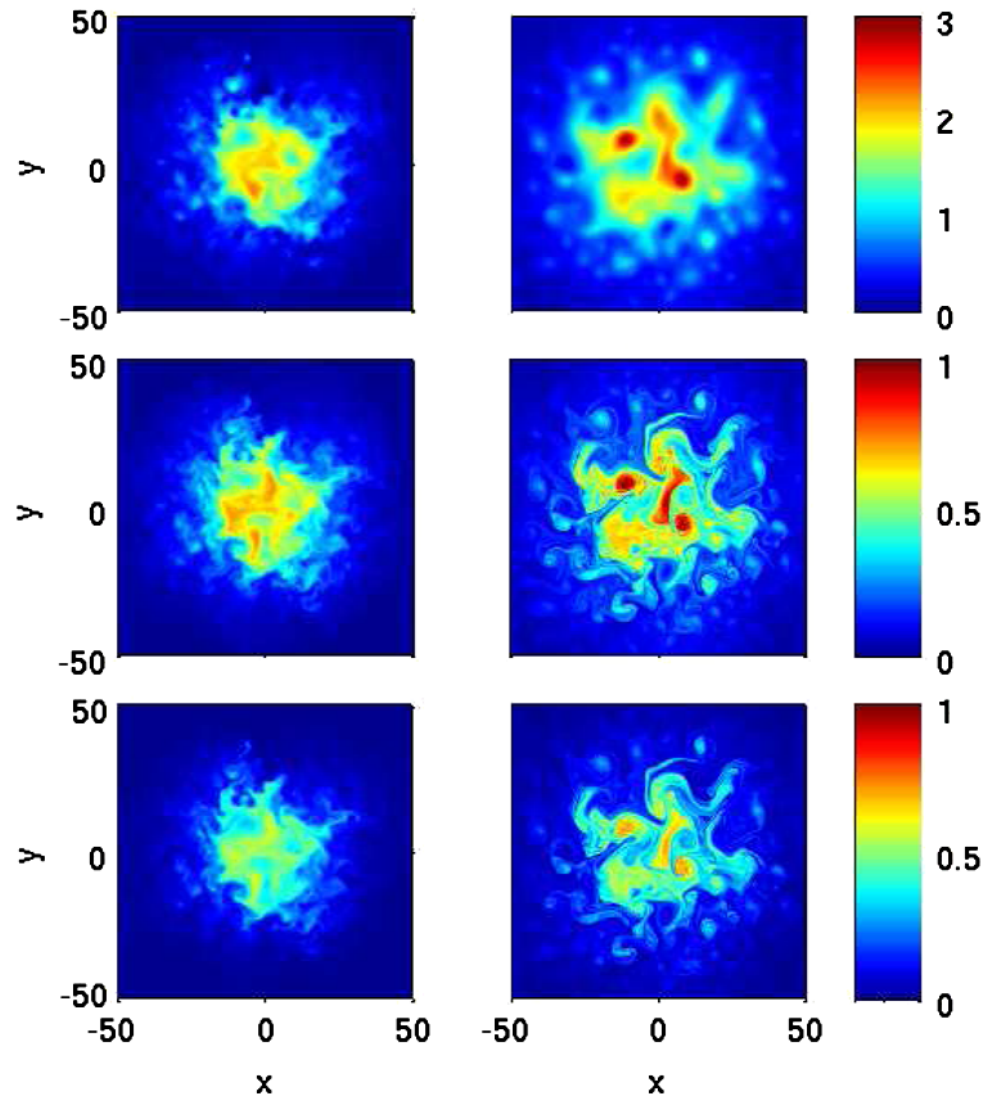
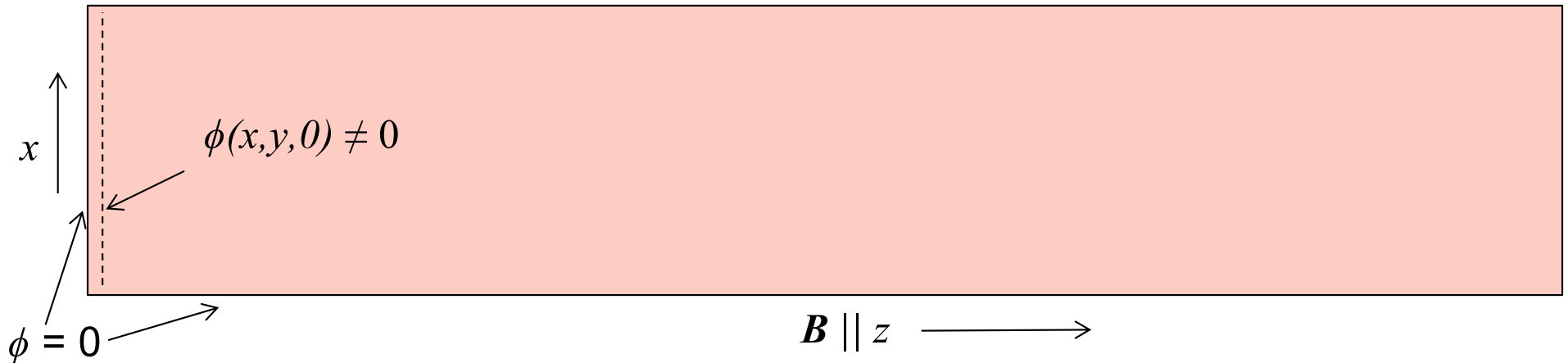


FIG. 1 (color online). Plots of  $\phi$  (top),  $T_e$  (center), and  $n$  (bottom) perpendicular to  $B$  in 3D (left) and 2D (right) simulations.

# Model Sheath Boundary Conditions

$$-\nabla_{\perp} \cdot (\epsilon_{\perp}(\vec{x}) \nabla_{\perp} \phi) = \sum_s q \int d^3v f$$



- GK Poisson Eq. solved in 2D planes at fixed  $z$ , only needs bcs on side walls (on  $x$  or  $y$  boundaries). Discontinuous jump between  $\phi(x, y, 0)$  just inside plasma and  $\phi=0$  end plates represents unresolved sheath. Determines reflected electrons:

$$f_e(x, y, 0, v_{\parallel}, \mu, t) = f_e(x, y, 0, -v_{\parallel}, \mu, t) \text{ for } 0 < v_{\parallel} < v_c \quad (1/2)mv_c^2 = q\phi_{\text{sheath}}$$

$$f_e(x, y, 0, v_{\parallel}, \mu, t) = 0 \quad \text{for } v_c < v_{\parallel}$$

- This is gyrokinetic version of electron sheath boundary condition used in early fluid edge simulations (Ricci, Rogers, et al., Friedman et al.), without assuming Maxwellian  $f$ . (Further generalizations possible in future.)
- Unlike some logical sheath models, allows  $j_{\parallel} \neq 0$ , in which case guiding center charge builds up and  $\phi$  in plasma rises. Allows currents to flow through walls.

## Energy Balance in SOL (with linearized polarization):

---

- If side walls at zero potential, then there is no energy input from ion polarization current to side walls. Total energy  $W_{tot}$  is sum of parallel kinetic energy and perpendicular ExB flow energy, which satisfies:

$$W_{tot} = \int d^3x \sum_s \int d^3v f(1/2) m v_{\parallel}^2 + \int d^3x \frac{\epsilon_{\perp}}{8\pi} |\nabla_{\perp} \phi|^2$$

$$dW_{tot}/dt = P_s - \int dS_{\parallel} \sum_s \int d^3v f(1/2) m v_{\parallel}^3 - \int dS_{\parallel} \phi j_{\parallel}$$

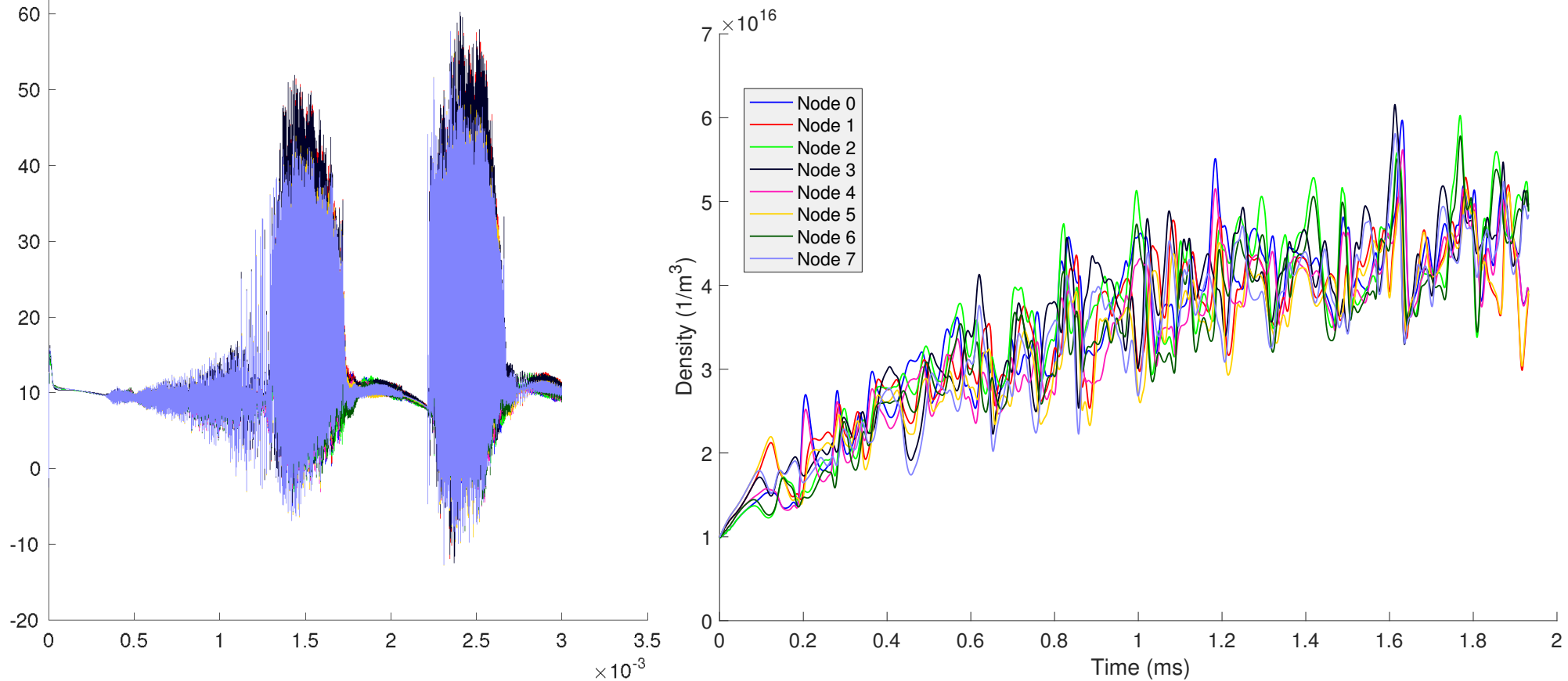
RHS represents (1) power input from the source, (2) kinetic energy flux to top of sheath, and (3) acceleration of ions and deceleration of electrons by sheath before they hit wall. If  $j_{\parallel}$  through the sheath is non-zero, puts energy into ExB flows.

# Initially worried about complications in interactions between sheaths ( $10^{11}$ Hz) & gyrokinetics ( $\sim 10^5$ Hz)

---

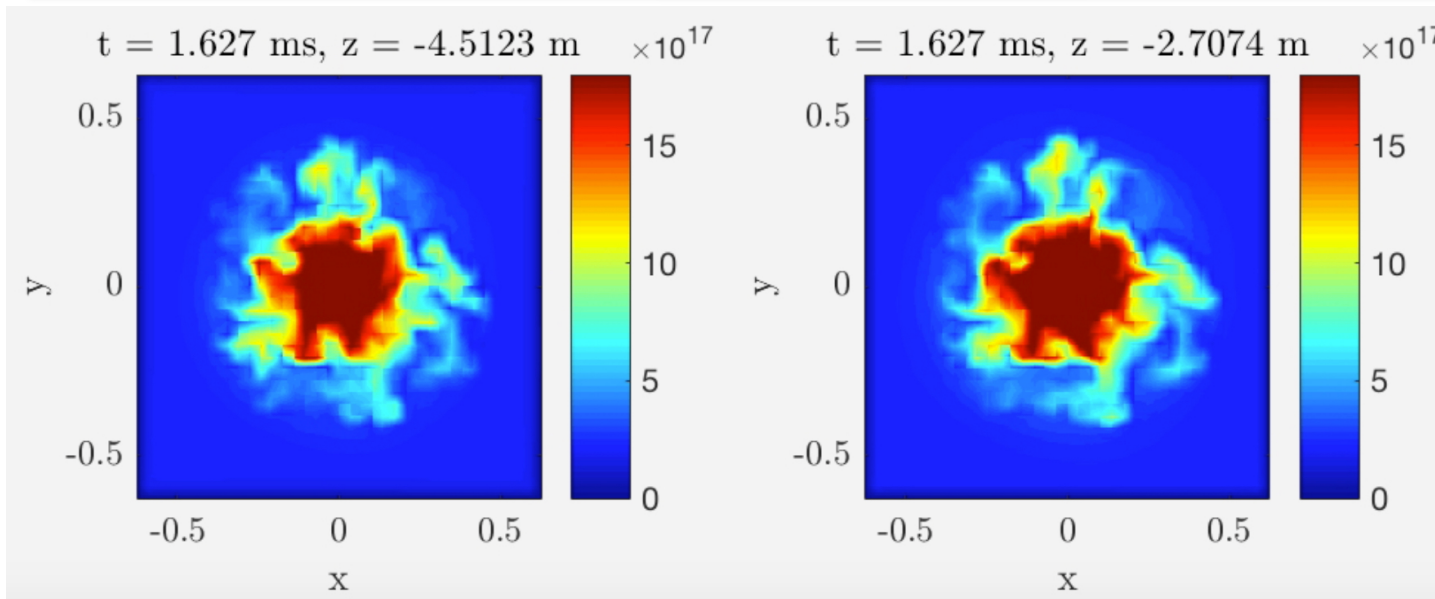
- In a gyrokinetic code, don't want to directly resolve tiny Debye-scale sheath ( $\sim 10^{-3}$  cm), evolves on extremely rapid time scale.
- “Logical sheath”: adjust phi at boundary to reflect most electrons and let through just enough electrons to match ion flux,  $j_{||} = 0$  (Parker, Procassini, Birdsall, Cohen 1993)
- Used in our 1D SOL ELM heat-pulse tests (Shi, Hakim, Hammett 2015), compares well with full PIC code, but how to interface with multi-dimensional GK?
- Eventually implemented gyrokinetic equivalent of sheath boundary conditions in early fluid edge simulations (Ricci, Rogers, GBS; Umansky, Friedman, BOUT++):
- Use GK Poisson eq. to determine potential everywhere in simulation, use jump between that at edge &  $\phi = 0$  plates to determine what fraction of electrons to reflect. Allows currents to flow into walls, steady state gives usual  $\phi_s \sim 3 T_e$ .
- Tried to increase side wall potential to avoid sharp gradients with sheath potential, was like biasing system with a power supply, drove huge potentials.
- Forgot collisions at first (because of previous ELM work), drives ultra-high frequencies
- Initially started with too much density near side walls, drove huge potentials.

# Some collisions needed for normal steady-state sheath



- Left: Collisionless simulation,  $\phi$  vs. time near simulation center, for a case with spatially uniform source. The potential is initially at a normal sheath level of  $\sim 3 T_e$ , but get huge, very-high-frequency oscillations after an ion connection time  $L_{||}/v_{ti} \sim 0.7$  ms.
- Right: Collisions included, density vs. time. Normal sheath & turbulence level.
- Sheath potential confines most electrons. Essential to have some collisions to scatter some electrons over the sheath barrier.

# First Gkeyll Simulation of 3D+2v Gyrokinetic Turbulence in Scrape Off Layer (SOL) / LAPD.



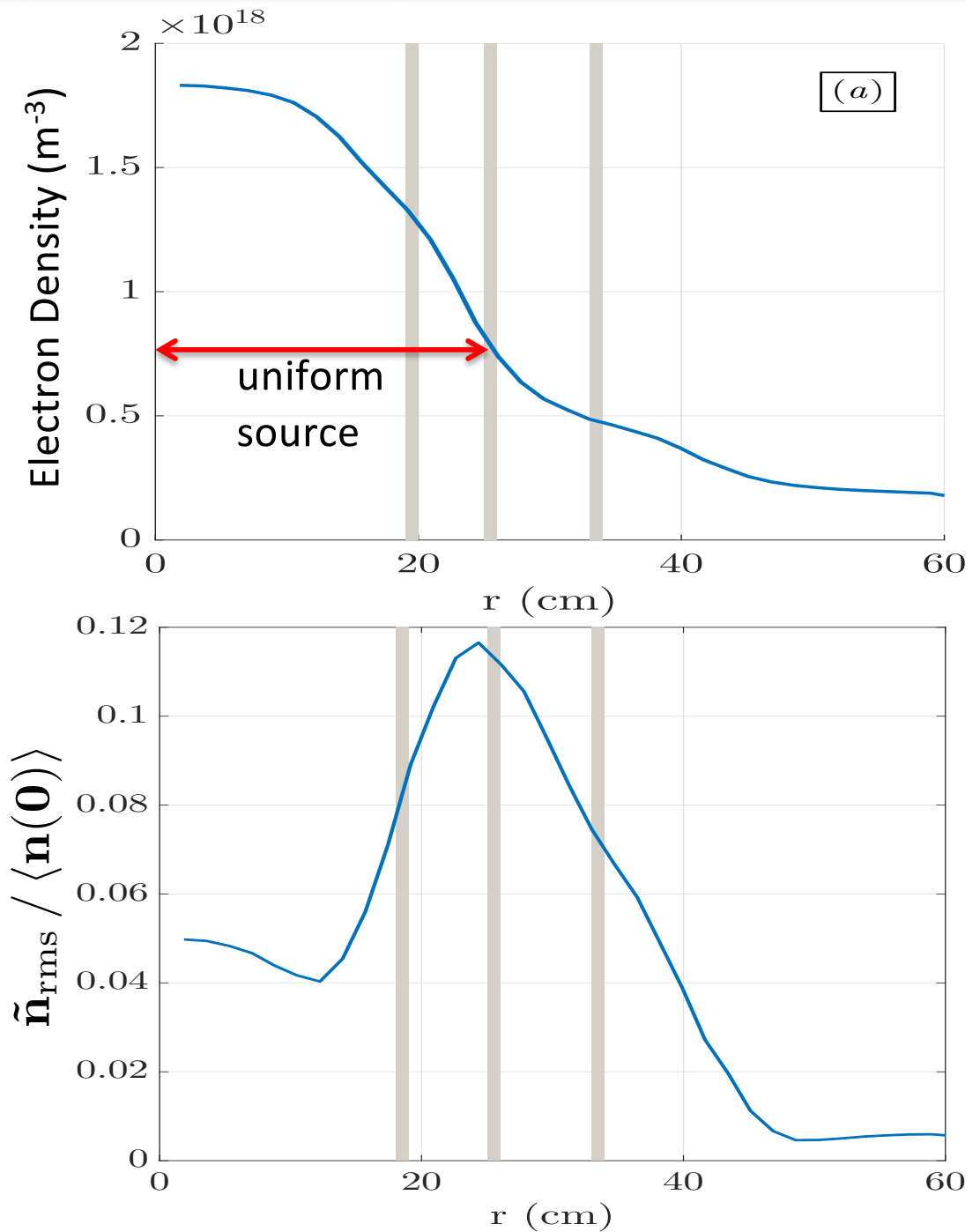
Density snapshots in LAPD simulation at 2 locations

- Was worried about difficulties in gyrokinetic-sheath interactions and other edge computational challenges. Indeed ran into & fixed several problems that drove high frequency, large amplitude fluctuations (special DG algorithms helped). Now appears fairly robust. (Working to reduce positivity and numerical heating issues.)
- Grid :  $N_x \times N_y \times N_z \times N_{v||} \times N_\mu = 36 \times 36 \times 10 \times 10 \times 5$  cells with 2 nodes in each dimension, approx. equiv. to  $72 \times 72 \times 20 \times 20 \times 10$  points (200 velocity grid points per spatial grid point).
- Gyrokinetic extension of pioneering fluid work (Rogers & Ricci, Umansky, Friedman et al.)

# Simulation of LAPD: strong turbulent transport

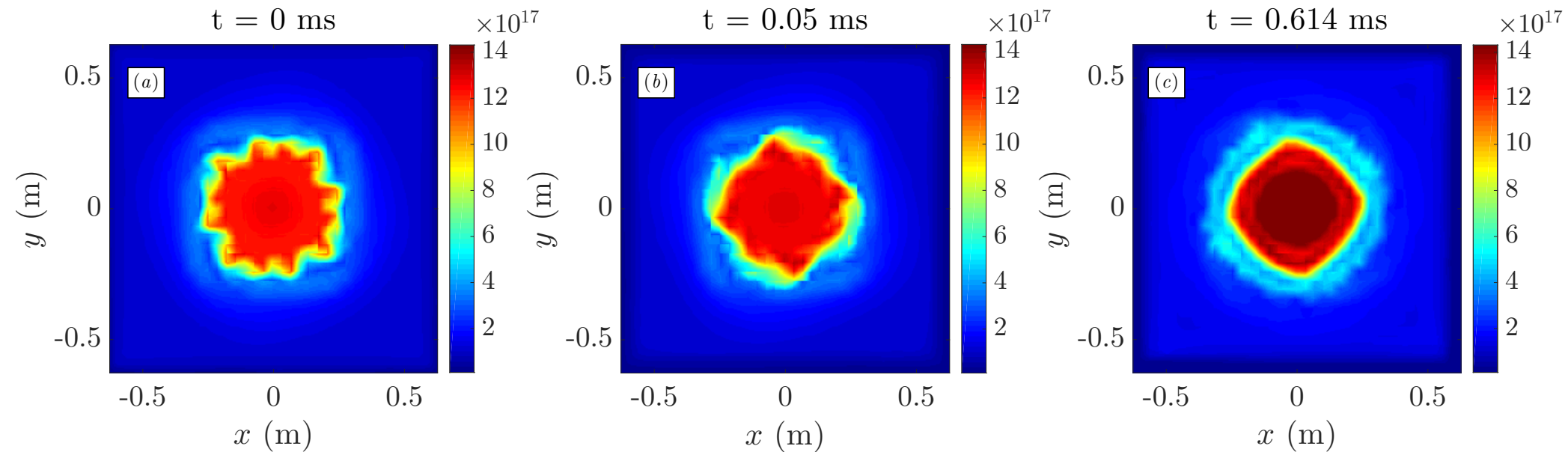
Turbulent fluctuations causes significant radial broadening of the density profile  $\langle n \rangle(r)$  relative to density source.

RMS fluctuation level in qualitative good agreement with LAPD observations (Friedman et al. PoP (2013)). (More precise simulations of specific experiment in future.)



# Simulations of biasing on LAPD

## show turbulence is quickly suppressed



- LAPD experiments with biasable limiter show suppression of turbulence by sheared rotation.<sup>1</sup>
- Can model limiter bias by modifying sheath boundary condition
- Starting from turbulent state, adding +20V biasing of limiter, simulation finds rapid suppression of turbulence

<sup>1</sup> Schaffner et al., PRL 2012

# Future positivity/energy improvements to DG algorithm & code

---

- Although DG limiters on boundary fluxes could ensure cell averaged positivity, the local density somewhere within a cell can go negative.
- Small diffusion used within a cell to restore positivity. This can add energy. Added an energy correction operator within the order of accuracy of the algorithm (similar to Taitano, Chacon, et al. JCP 2015).
- At present, still have some numerical heating near the end plates where  $T_{\parallel}$  gets smaller than the minimum energy representable on  $\mu$  ( $v_{\perp}$ ) grid, when collision operator tries to isotropize.
- Can be fixed in the future with non-uniform  $\mu$  grid, or with exponential-basis functions (which have no limit on minimum energy).
- Other algorithmic improvements: super-time-stepping / implicit collision operator, exponential basis functions, sparse quadrature methods to reduce number of basis functions in high dimensions...

# Sparse Grid Methods Might Give Major Speedup to DG

---

- Consider piecewise parabolic DG basis functions in each cell, in 1 D:

$$f(x) = f_0 + f_1x + f_2x^2.$$

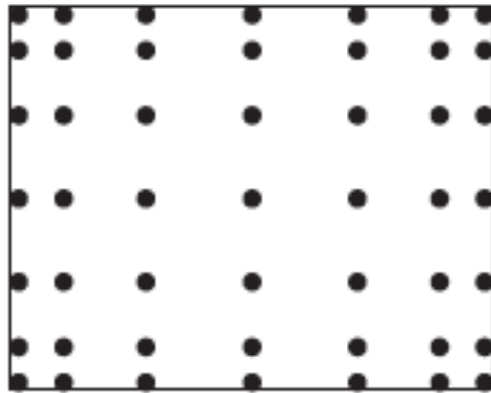
- Straightforward Lagrange tensor product for gyrokinetics, with 3 points in each dimension has  $3^5 = 243$  points per cell.
- But this involves terms up to 10th order,  $O((\Delta x)^2(\Delta y)^2(\Delta z)^2(\Delta v_{||})^2(\Delta \mu)^2)$ , most of which can't matter to the accuracy of the algorithm.
- Keeping only terms through 2nd order **reduces number of basis functions per cell by more than a factor of 10.**
- Related to sparse-grid quadrature. Some initial work in Applied Math community on combining with DG, requires more research to work out details, tricks for energy conservation, how to best implement, ...

# Sparse Grid Methods Should Give Major Speedup to DG

standard 7x7 grid

Product rule:

$$\mathbb{X}_3 \otimes \mathbb{X}_3$$

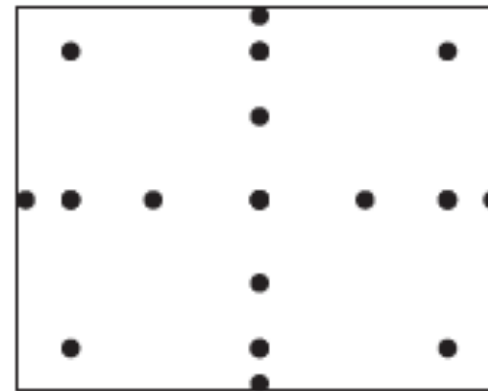


2D  
6<sup>th</sup> order  
example:

Equivalent sparse grid with same order of accuracy:

Sparse grid:

$$\mathbb{X}_{2,3}$$



5D  
2<sup>nd</sup> order  
case:

Standard 2<sup>nd</sup> order basis functions requires 3 points in each direction:  
 $3^5 = 243$  points total

Equivalent order of accuracy sparse basis functions can be represented with only 21 points, ~10x savings.

# Conclusions

---

- First results from Gkeyll code of 5D continuum gyrokinetic simulations on open field lines with model sheath boundary conditions.
- Simulation of LAPD-like configuration shows density fluctuation levels in the right ballpark. Have also done TORPEX/Helimak type geometry with bad curvature drive of toroidal magnetic field.
- Using various simplifications at present, such as simple helical magnetic field model without separatrix, but sufficient to demonstrate feasibility of approach and contains some key physics of the SOL (such as bad curvature drive of toroidal instabilities, rapid parallel losses to divertor plates and interactions with sheaths).
- Could begin physics studies about the nature of SOL turbulence, such as:  
Why doesn't this turbulence spread power more widely on divertor plates.  
What are effects of reduced recycling with lithium?
- Future work: More detailed atomic physics, viscosity from neutral. Extensions to general geometry to handle open and closed field lines simultaneously with a separatrix. Algorithmic improvements.